Available online at http://scik.org
Commun. Math. Biol. Neurosci. 2022, 2022:72
https://doi.org/10.28919/cmbn/7516
ISSN: 2052-2541

FRACTAL-FRACTIONAL SIRS EPIDEMIC MODEL WITH TEMPORARY IMMUNITY USING ATANGANA-BALEANU DERIVATIVE

ERIC OKYERE[1,2,*], BABA SEIDU[1], KWARA NANTOMAH[1], JOSHUA KIDDY K. ASAMOAH[3]

[1]Department of Mathematics, C. K. Tedam University of Technology and Applied Sciences, Navrongo, Ghana

[2]Department of Mathematics and Statistics, University of Energy and Natural Resources, Sunyani, Ghana

[3]Department of Mathematics, Kwame Nkrumah University of Science and Technology, Kumasi, Ghana

Abstract. The basic SIRS deterministic model is one of the powerful and important compartmental modeling frameworks that serve as the foundation for a variety of epidemiological models and investigations. In this study, a nonlinear Atangana-Baleanu fractal-fractional SIRS epidemiological model is proposed and analysed. The model's equilibrium points (disease-free and endemic) are studied for local asymptotic stability. The existence of the model's solution and its uniqueness, as well as the Hyers-Ulam stability analysis, are established. Numerical solutions and phase portraits for the fractal-fractional model are generated using a recently constructed and effective Newton polynomial-based iterative scheme for nonlinear dynamical fractal-fractional model problems. Our numerical simulations demonstrate that fractal-fractional dynamic modeling is a very useful and appropriate mathematical modeling tool for developing and studying epidemiological models.

Keywords: SIRS deterministic model; Atangana-Baleanu fractal-fractional derivative; Newton polynomial; existence and uniqueness.

2010 AMS Subject Classification: 34A08, 26A33, 37N25.

*Corresponding author
E-mail address: eric.okyere@uenr.edu.gh
Received May 20, 2022

1. Introduction

Mathematical modeling is a useful tool for describing and studying various aspects of real-world problems by constructing realistic models, which are critical in the development of methods for preventing, controlling, and mitigating the impacts of infectious diseases. In mathematical modeling of infectious diseases, the compartmental framework is constructed based on the characteristics of the disease being studied as well as the objective of the model [1]. In the literature of epidemiological modeling utilizing differential equations, the classical SI, SIS, SIR, SIRS, and SEIR compartmental formulations have served as the foundation for a variety of epidemiological models and investigations. Integer-order differential equations have been widely used in the mathematical modeling framework of infectious diseases and real-world engineering applications. Despite its vast applications in compartmental epidemiological modeling and other engineering applications, several authors continue to utilize these types of equations to develop and analyze their mathematical models [2, 3, 4, 5, 6, 7, 8, 9, 1, 10, 11]. However in recent years, the concept and application of fractional order calculus in mathematical modeling in science and engineering has become an intriguing research subject, as evidenced by the number of significant papers and written textbooks in recent literature [12, 13, 14, 15, 16, 17, 18, 19, 20, 21, 22, 23, 24, 25]. In a study by Omame et al. [26], the Atangana-Baleanu derivative was used to construct and analyze a data-driven COVID-19 and tuberculosis co-infection non-integer mathematical model. They established the global asymptotic stability of the disease-free steady state for this new co-infection dynamical model. In a recent study, Khan and his co-workers [27] utilized Atangana-Baleanu-Caputo and Liouville-Caputo derivatives to introduce and analyze HIV/AIDS nonlinear fractional order epidemiological models. Khan and Atangana [28] constructed and parameterized a deterministic epidemiological model based on the available infection cases of COVID-19 outbreaks in Wuhan, China. They gave some analytical results on the initial constructed integer order model, as well as numerical simulations for the Atangana-Baleanu type dynamical model for this contagious disease. Bonyah et al. [29] formulated and analyzed an ABC fractional operator type human African trypanosomiasis model, as well as providing numerical results.

Fractal-fractional differential equations with fractal-fractional derivative operators are new powerful and more efficient mathematical modeling tools [30, 31, 32, 33, 34]. These new approaches of fractional differentiation and integration that captures fractal dynamics are based on the generalized Mittag-Leffler law, exponential decay law and power law kernel operators recently studied by Atangana [35]. Several recent studies have established that the use of fractal-fractional order derivatives to develop and analyze nonlinear mathematical models within compartmental epidemiological frameworks is suitable and generates realistic results. For instance, the analysis of the Hepatitis B virus with asymptomatic class using both fractional and fractal-fractional order Atangana-Baleanu operators in the Caputo sense is detailed in a study by Zhang et al. [36]. Khan and his co-authors [37] generated some illustrative numerical solutions for their proposed fractal-fractional COVID-19 mathematical model using a recently established Newton polynomial based iterative scheme for Atangana-Baleanu fractal-fractional type dynamical models. A nonlinear $S_hE_hA_hI_hR_hS_vE_vI_v$ deterministic fractal-fractional dengue fever mathematical model constructed with Atangana-Baleanu derivative is studied by El-Dessoky [38]. Ghanbari and Gómez-Aguilar [39] considered detailed analysis and numerical approximations of two avian influenza fractal-fractional nonlinear models using the power law kernel and the generalized Mittag-Leffler kernel operators. Based on the classical deterministic competition model, Wang and Khan [40], Atangana et al. [41], and Li et al. [42] have constructed nonlinear fractal-fractional models to study the competition dynamics among commercial and rural banks in Indonesia using the same data range (2004-2014). Fractal-fractional deterministic compartmental models have been proposed and analysed to gain more insight into the transmission of the very recent COVID-19 outbreak [43, 44, 45, 46, 47, 48, 49, 50, 51, 52].Using deterministic compartmental modeling frameworks, Ali et al. [53] and Li et al. [54] formulated and examined fractal-fractional dynamical models of the highly infectious HIV/AIDS disease. The author of [55] presented on the mathematical modeling of the interplay between the immune system and tumor progression utilizing three different fractional and fractal-fractional order derivatives. In 2021, the authors of [56] formulated and investigated a fractal-fractional mathematical model for cervical cancer. Recently, Asamoah [57] studied a deterministic nonlinear fractal-fractional Q fever epidemic modeling, analysis, and numerical approximations. Also, the work in [58] studied a fractal-fractional model for $CD4^+$ T-Cells under the effect of HIV-1 Infection.

This study has two primary objectives. The first objective is to extend and generalize Hethcote's [59] non-fractional order deterministic SIRS epidemic model by utilizing the Atangana–Baleanu fractal-fractional derivative operator. The second objective is to present numerical solutions to the proposed model and also provide phase portrait plots for some selected values of the fractal and fractional orders using a Newton polynomial iterative scheme. Our new work is motivated by the classical SIRS epidemiological model, which was constructed and studied by Hethcote [59]. In addition, the aforementioned literature, the Atangana-Baleanu fractal-fractional derivative, as well as the novel Newton polynomial iterative scheme [60], have motivated our present mathematical modeling investigation.

The remaining sections of the study are organized as follows. Section 2 covers the essential preliminaries for the fractal-fractional derivative and integral. Section 3 is concerned with formulating the non-integer order fractal-fractional SIRS model, of which we will begin with a brief overview of the integer-order SIRS model. We will explore the model's equilibrium points (disease-free and endemic) local asymptotic stability in section 4. The existence of the model's solution and its uniqueness, as well as the Hyers-Ulam stability analysis, will be considered in sections 5, 6, and 7 respectively. In section 8, we will provide a brief introduction of the numerical scheme that will be utilized to compute the model's numerical solutions and also generate phase portrait graphs. We will further discuss the numerical simulation results in the same section. Finally, we will conclude the study in section 9.

2. Some Important Definitions and Preliminaries

Definition 2.1. [35] Given that $f(t)$ is a continuous function and fractal differentiable on an open (a,b) with order δ_2 then the fractal-fractional derivative of $f(t)$ with order δ_1 in the Caputo sense having the generalized Mittag-Leffler type kernel is defined as follows:

$$ {}_{0}^{FF}D_t^{\delta_1,\delta_2} f(t) = \frac{AB(\delta_1)}{1-\delta_1} \int_0^t \frac{d}{d\psi^{\delta_2}} f(\psi) E_{\delta_1}\left(-\frac{\delta_1}{1-\delta_1}(t-\psi)^{\delta_1}\right) d\psi . \tag{1}$$

where $0 < \delta_1, \delta_2 \leq 1$ and $AB(\delta_1) = 1 - \delta_1 + \frac{\delta_1}{\Gamma(\delta_1)}$.

Definition 2.2. [35] The fractal-fractional integral of a continuous function $f(t)$ involving the generalized Mittag-Leffler type kernel is defined as

$$ {}_0^{FF}I_t^{\delta_1,\delta_2} f(t) = \frac{\delta_2(1-\delta_1)t^{\delta_2-1}}{AB(\delta_1)} f(t) + \frac{\delta_1\delta_2}{AB(\delta_1)\Gamma(\delta_1)} \int_0^t \psi^{\delta_2-1} f(\psi)(t-\psi)^{\delta_1-1} d\psi. \tag{2}$$

3. Model Formulation

In this section, we will formulate and analyze a new fractal-fractional SIRS epidemiological model characterized by the Atangana-Baleanu derivative. We will begin by providing a brief overview of the classical SIRS model that assumes constant population dynamics [59]. This compartmental model captures temporary immunity and also assumes equal vital dynamics (birth and death rates). The population is categorized into three groups: Susceptible Individuals, Infective Individuals, and Recovered Individuals, each with a population size of $\tilde{S}(t)$,$\tilde{I}(t)$, and $\tilde{R}(t)$ respectively.

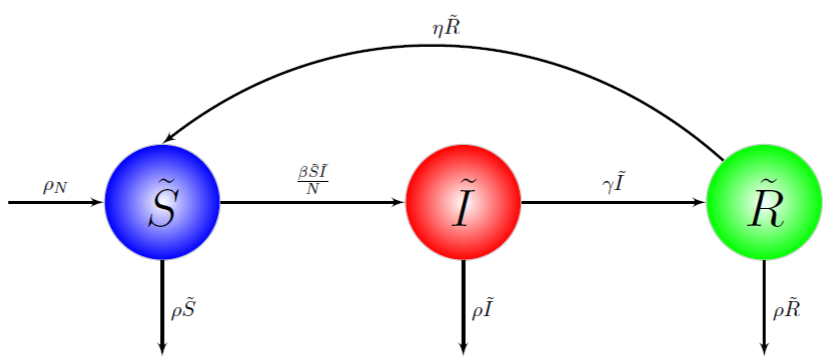

FIGURE 1. Flow diagram for the classical SIRS model with constant population dynamics where β, γ, and η represent the infection rate, removal rate, and loss of immunity rate, respectively. The model parameter ρ represent birth rate and natural death rate.

Following the SIRS compartmental structure as shown above, the deterministic integer-order initial value problem is given below:

$$\begin{aligned}\frac{d\tilde{S}}{dt} &= \rho N + \eta \tilde{R}(t) - \frac{\beta \tilde{S}(t)\tilde{I}(t)}{N} - \rho \tilde{S}(t),\\ \frac{d\tilde{I}}{dt} &= \frac{\beta \tilde{S}(t)\tilde{I}(t)}{N} - \gamma \tilde{I}(t) - \rho \tilde{I}(t),\\ \frac{d\tilde{R}}{dt} &= \gamma \tilde{I}(t) - \eta \tilde{R}(t) - \rho \tilde{R}(t),\end{aligned} \tag{3}$$

where $\tilde{S}(t)+\tilde{I}(t)+\tilde{R}(t)=N$ and initial conditions: $\tilde{S}\geq 0,\ \tilde{I}\geq 0,\ \tilde{R}\geq 0$.

Now, we re-write the model problem in terms of the proportions of susceptible, infective, and recovered individuals. For this purpose, we introduce the following new variables that represent the proportions of the various sub-populations.

Let $S=\frac{\tilde{S}}{N}$, $I=\frac{\tilde{I}}{N}$ and $R=\frac{\tilde{R}}{N}$, so that $S+I+R=1$.

Therefore knowing that $R=1-S-I$, the model (3) becomes

$$\begin{aligned}\frac{dS}{dt} &= (\rho+\eta) - \beta S(t)I(t) - \eta I(t) - (\rho+\eta)S(t),\\ \frac{dI}{dt} &= \beta S(t)I(t) - \gamma I(t) - \rho I(t),\end{aligned} \tag{4}$$

where $R(t)=1-S(t)-I(t)$.

Now, we utilized the fractal-fractional derivative operator defined above to generalize the integer-order deterministic SIRS mathematical model (4) to obtain an Atanagana-Baleanu type fractal-fractional dynamical model. It then follows that our proposed fractal-fractional SIRS model with constant population dynamics takes the form given below:

$$\begin{aligned}{}_0^{FF}D_t^{\delta_1,\delta_2} S(t) &= (\rho+\eta) - \beta S(t)I(t) - \eta I(t) - (\rho+\eta)S(t),\\ {}_0^{FF}D_t^{\delta_1,\delta_2} I(t) &= \beta S(t)I(t) - \gamma I(t) - \rho I(t).\end{aligned} \tag{5}$$

4. Model Equilibria and Local Stability Analysis

We can easily deduce from the basic concepts in compartmental modeling of infectious diseases that the basic reproduction number ($\mathscr{R}_0$) for this mathematical model is given by $\mathscr{R}_0=\frac{\beta}{\gamma+\rho}$.

Let

$$
\begin{cases} {}_{0}^{FF}D_t^{\delta_1,\delta_2}S(t) = 0, \\ {}_{0}^{FF}D_t^{\delta_1,\delta_2}I(t) = 0. \end{cases} \tag{6}
$$

Now, by solving equation (6) without showing the steps involved, the model equilibria are given as follows:

$DE_0 = (1,0)$ and $EE^* = \left(\frac{1}{\mathscr{R}_0}, \frac{(\rho+\eta)(\mathscr{R}_0 - 1)}{\beta + \eta\mathscr{R}_0}\right)$.

where DE_0 is the disease-free equilibrium point and EE^* represent the endemic equilibrium point.

4.1. Local Stablity of DE_0.

Theorem 4.1. *The equilibrium point DF_o of the nonlinear Atangana-Baleanu fractal-fractional SIRS model (5) is locally asymptotically stable if $\mathscr{R}_0 > 1$.*

Proof. By computing the SIRS initial value problem's Jacobian matrix and evaluating it at the equilibrium point DE_0, we obtain the simplified Jacobian matrix given below

$$
J(DE_0) = \begin{bmatrix} -(\rho+\eta) & -\beta-\eta \\ & \\ 0 & \beta-(\gamma+\rho) \end{bmatrix}. \tag{7}
$$

The eigenvalues for the 2×2 upper triangular Jacobian matrix are $\lambda_1 = -(\rho+\eta)$ and $\lambda_2 = \beta - (\gamma+\rho)$. It is not difficult to conclude that $\lambda_1 < 0$. Now for the second eigenvalue to have negative real part, then we have

$$
\lambda_2 = \beta - (\gamma+\rho) < 0 \Longrightarrow \frac{\beta}{\gamma+\rho} < 1.
$$

We can therefore say that, λ_2 will have negative real part provided $\mathscr{R}_0 = \frac{\beta}{\gamma+\rho} < 1$.
Following this analysis, we conclude that DE_0 is locally asymptotically stable. □

4.2. Local Stablity of EE^*.

Theorem 4.2. *The equilibrium point EE^* of the nonlinear Atangana-Baleanu fractal-fractional SIRS model (5) is locally asymptotically stable if $\mathscr{R}_0 > 1$.*

Proof. The simplified Jacobian matrix given below is obtained by computing the SIRS initial value problem's Jacobian matrix and evaluating it at the equilibrium, EE^*.

$$J(EE^*) = \begin{bmatrix} -\dfrac{\beta(\rho+\eta)(\mathscr{R}_0-1)}{(\beta+\eta\mathscr{R}_0)} - (\rho+\eta) & -(\gamma+\rho+\eta) \\ \\ \dfrac{\beta(\rho+\eta)(\mathscr{R}_0-1)}{(\beta+\eta\mathscr{R}_0)} & 0 \end{bmatrix}. \tag{8}$$

Now, to ensure that the derived endemic equilibrium, EE^* is locally asymptotically stable, the two eigenvalues of $J(EE^*)$ must have negative real components. This condition will hold true if the Routh-Hurwitz stability criteria for the characteristic equation of the computed Jacobian matrix are satisfied.
The characteristic equation associated with matrix $J(EE^*)$ is given by

$$\lambda^2 + d_1\lambda + d_2 = 0, \tag{9}$$

where

$$d_1 = \frac{\beta(\rho+\eta)(\mathscr{R}_0-1)}{(\beta+\eta\mathscr{R}_0)} + (\rho+\eta),$$
$$d_2 = \frac{\beta(\rho+\eta)(\gamma+\rho+\eta)(\mathscr{R}_0-1)}{(\beta+\eta\mathscr{R}_0)}.$$

Since $\mathscr{R}_0 > 1$, it follows that $d_1 > 0$ and $d_2 > 0$. Hence, the Routh-Hurwitz stability conditions are satisfied. This completes the proof. □

5. Existence Criteria

In this part of our mathematical modeling analysis, we consider and investigate the existence of the fractal-fractal model solution. For this purpose, we apply the fixed point theory and utilizing the fractal-fractional integral operator (2), the constructed model problem (5) is converted into an integral equation as given below.

$$
\begin{aligned}
S(t)-S(0) &= \frac{\delta_2(1-\delta_1)t^{\delta_2-1}}{AB(\delta_1)}\Big((\rho+\eta)-\beta SI-\eta I-(\rho+\eta)S\Big) \\
&+ \frac{\delta_1\delta_2}{AB(\delta_1)\Gamma(\delta_1)}\int_0^t \psi^{\delta_2-1}(t-\psi)^{\delta_1-1}\Big((\rho+\eta)-\beta SI-\eta I-(\rho+\eta)S\Big)\,d\psi, \\
I(t)-I(0) &= \frac{\delta_2(1-\delta_1)t^{\delta_2-1}}{AB(\delta_1)}\Big(\beta SI-\gamma I-\rho I\Big) \\
&+ \frac{\delta_1\delta_2}{AB(\delta_1)\Gamma(\delta_1)}\int_0^t \psi^{\delta_2-1}(t-\psi)^{\delta_1-1}\Big(\beta SI-\gamma I-\rho I\Big)\,d\psi.
\end{aligned} \tag{10}
$$

We now define some functions W_1 and W_2 given as follows:

$$
\begin{aligned}
W_1(t,S) &= (\rho+\eta)-\beta S(t)I(t)-\eta I(t)-(\rho+\eta)S(t), \\
W_2(t,I) &= \beta S(t)I(t)-\gamma I(t)-\rho I(t).
\end{aligned}
$$

We need the following assumptions to help us derive our results:

(Q^*) : Let assume that $S^*(t),\ I^*(t),\ S(t)$ and $I(t)$ are bounded functions such that $\|S(t)\| \le \xi_1$, $\|I(t)\| \le \xi_2$.

Theorem 5.1. *If the assumption (Q^*) holds true then the kernels W_1 and W_2 satisfies the Lipschitz condition and are contractions provided the following inequality holds*

$$0 \le \varphi_i < 1, \quad i = 1,\ 2.$$

Proof.

$$
\begin{aligned}
\|W_1(t,S)-W_1(t,S^*)\| =& \Big\|\Big((\rho+\eta)-\beta SI-\eta I-(\rho+\eta)S\Big) \\
&-\Big((\rho+\eta)-\beta S^*I-\eta I-(\rho+\eta)S^*\Big)\Big\| \\
=& \Big\|-\beta I\Big(S-S^*\Big)-(\rho+\eta)\Big(S-S^*\Big)\Big\| \\
\le& \Big(\beta\|I\|+\rho+\eta\Big)\Big\|\Big(S-S^*\Big)\Big\| \\
\le& \varphi_1\Big\|\Big(S-S^*\Big)\Big\|, \qquad (11)
\end{aligned}
$$

where $\varphi_1 = \beta\xi_2 + \rho + \eta$.

$$
\begin{aligned}
\left\|W_2(t,I) - W_2(t,I^*)\right)\| &= \left\|\left(\beta SI - \gamma I - \rho I\right) - \left(\beta SI^* - \gamma I^* - \rho I^*\right)\right\| \\
&= \left\|\beta S\left(I - I^*\right) - (\gamma + \rho)\left(I - I^*\right)\right\| \\
&\leq \left(\beta\|S\| + \gamma + \rho\right)\left\|\left(I - I^*\right)\right\| \\
&\leq \varphi_2\left\|\left(I - I^*\right)\right\|,
\end{aligned} \tag{12}
$$

where $\varphi_2 = \beta\xi_1 + \gamma + \rho$. □

Knowing the expressions for the two functions W_1 and W_2 and also assuming the initial conditions $S(0) = I(0) = 0$, we can rewrite equation (10) in a more simplified form as follows:

$$
\begin{aligned}
S(t) &= \frac{\delta_2(1-\delta_1)t^{\delta_2-1}}{AB(\delta_1)} W_1\left(t, S(t)\right) + \frac{\delta_1\delta_2}{AB(\delta_1)\Gamma(\delta_1)} \int_0^t \psi^{\delta_2-1}(t-\psi)^{\delta_1-1} W_1\left(\psi, S(\psi)\right) d\psi, \\
I(t) &= \frac{\delta_2(1-\delta_1)t^{\delta_2-1}}{AB(\delta_1)} W_2\left(t, I(t)\right) + \frac{\delta_1\delta_2}{AB(\delta_1)\Gamma(\delta_1)} \int_0^t \psi^{\delta_2-1}(t-\psi)^{\delta_1-1} W_2\left(\psi, I(\psi)\right) d\psi.
\end{aligned} \tag{13}
$$

Recursively, equation (13) becomes

$$
\begin{aligned}
S_n(t) &= \frac{\delta_2(1-\delta_1)t^{\delta_2-1}}{AB(\delta_1)} W_1\left(t, S_{n-1}(t)\right) + \frac{\delta_1\delta_2}{AB(\delta_1)\Gamma(\delta_1)} \int_0^t \psi^{\delta_2-1}(t-\psi)^{\delta_1-1} W_1\left(\psi, S_{n-1}(\psi)\right) d\psi, \\
I_n(t) &= \frac{\delta_2(1-\delta_1)t^{\delta_2-1}}{AB(\delta_1)} W_2\left(t, I_{n-1}(t)\right) + \frac{\delta_1\delta_2}{AB(\delta_1)\Gamma(\delta_1)} \int_0^t \psi^{\delta_2-1}(t-\psi)^{\delta_1-1} W_2\left(\psi, I_{n-1}(\psi)\right) d\psi.
\end{aligned} \tag{14}
$$

Now considering the difference between recursive expressions we obtain

$$
\begin{aligned}
DS_{n+1}(t) &= S_{n+1} - S_n \\
&= \frac{\delta_2(1-\delta_1)t^{\delta_2-1}}{AB(\delta_1)} W_1\left(t, S_n(t)\right) + \frac{\delta_1\delta_2}{AB(\delta_1)\Gamma(\delta_1)} \int_0^t \psi^{\delta_2-1}(t-\psi)^{\delta_1-1} W_1\left(\psi, S_n(\psi)\right) d\psi \\
&- \left(\frac{\delta_2(1-\delta_1)t^{\delta_2-1}}{AB(\delta_1)} W_1\left(t, S_{n-1}(t)\right) + \frac{\delta_1\delta_2}{AB(\delta_1)\Gamma(\delta_1)} \int_0^t \psi^{\delta_2-1}(t-\psi)^{\delta_1-1} W_1\left(\psi, S_{n-1}(\psi)\right) d\psi\right) \\
&= \frac{\delta_2(1-\delta_1)t^{\delta_2-1}}{AB(\delta_1)} \left(W_1\left(t, S_n(t)\right) - W_1\left(t, S_{n-1}(t)\right)\right) \\
&\quad + \frac{\delta_1\delta_2}{AB(\delta_1)\Gamma(\delta_1)} \int_0^t \psi^{\delta_2-1}(t-\psi)^{\delta_1-1} \left(W_1\left(\psi, S_n(\psi)\right) - W_1\left(\psi, S_{n-1}(\psi)\right)\right) d\psi,
\end{aligned}
$$

$$
\begin{aligned}
DI_{n+1}(t) &= I_{n+1} - I_n \\
&= \frac{\delta_2(1-\delta_1)t^{\delta_2-1}}{AB(\delta_1)} W_2\Big(t, I_n(t)\Big) + \frac{\delta_1\delta_2}{AB(\delta_1)\Gamma(\delta_1)} \int_0^t \psi^{\delta_2-1}(t-\psi)^{\delta_1-1} W_2\Big(\psi, I_n(\psi)\Big)\, d\psi \\
&- \left(\frac{\delta_2(1-\delta_1)t^{\delta_2-1}}{AB(\delta_1)} W_2\Big(t, I_{n-1}(t)\Big) + \frac{\delta_1\delta_2}{AB(\delta_1)\Gamma(\delta_1)} \int_0^t \psi^{\delta_2-1}(t-\psi)^{\delta_1-1} W_2\Big(\psi, I_{n-1}(\psi)\Big)\, d\psi\right) \\
&= \frac{\delta_2(1-\delta_1)t^{\delta_2-1}}{AB(\delta_1)} \Big(W_2\Big(t, I_n(t)\Big) - W_2\Big(t, I_{n-1}(t)\Big)\Big) \\
&\quad + \frac{\delta_1\delta_2}{AB(\delta_1)\Gamma(\delta_1)} \int_0^t \psi^{\delta_2-1}(t-\psi)^{\delta_1-1} \Big(W_2\Big(\psi, I_n(\psi)\Big) - W_2\Big(\psi, I_{n-1}(\psi)\Big)\Big)\, d\psi.
\end{aligned}
$$

Taking the norms of the above recursive differences we have

$$
\begin{aligned}
\big\|DS_{n+1}(t)\big\| &= \big\|S_{n+1} - S_n\big\| \\
&= \Bigg\| \frac{\delta_2(1-\delta_1)t^{\delta_2-1}}{AB(\delta_1)} \Big(W_1\Big(t, S_n(t)\Big) - W_1\Big(t, S_{n-1}(t)\Big)\Big) \\
&\qquad + \frac{\delta_1\delta_2}{AB(\delta_1)\Gamma(\delta_1)} \int_0^t \psi^{\delta_2-1}(t-\psi)^{\delta_1-1} \Big(W_1\Big(\psi, S_n(\psi)\Big) - W_1\Big(\psi, S_{n-1}(\psi)\Big)\Big)\, d\psi \Bigg\|,
\end{aligned}
$$

$$
\begin{aligned}
\big\|DI_{n+1}(t)\big\| &= \big\|I_{n+1} - I_n\big\| \\
&= \Bigg\| \frac{\delta_2(1-\delta_1)t^{\delta_2-1}}{AB(\delta_1)} \Big(W_2\Big(t, I_n(t)\Big) - W_2\Big(t, I_{n-1}(t)\Big)\Big) \\
&\qquad + \frac{\delta_1\delta_2}{AB(\delta_1)\Gamma(\delta_1)} \int_0^t \psi^{\delta_2-1}(t-\psi)^{\delta_1-1} \Big(W_2\Big(\psi, I_n(\psi)\Big) - W_2\Big(\psi, I_{n-1}(\psi)\Big)\Big)\, d\psi \Bigg\|.
\end{aligned}
$$

Theorem 5.2. *The non-integer deterministic Atangana-Baleanu type compartmental model (5) has a solution provided the inequality below holds true:*

$$\kappa = max\{\varphi_1,\ \varphi_2\} < 1.$$

Proof. We define two functions $Z_{1n}(t)$ and $Z_{2n}(t)$ given by

$$Z_{1n}(t) = S_{n+1}(t) - S(t), \tag{15}$$

$$Z_{2n}(t) = I_{n+1}(t) - I(t). \tag{16}$$

By taking the norm of the function $Z_{1n}(t)$ defined above we obtain

$$\begin{aligned}
\left\|Z_{1n}(t)\right\| &= \left\|S_{n+1}-S\right\| \\
&= \Bigg\| \frac{\delta_2(1-\delta_1)t^{\delta_2-1}}{AB(\delta_1)}\Big(W_1\big(t,S_n(t)\big)-W_1\big(t,S(t)\big)\Big) \\
&\qquad + \frac{\delta_1\delta_2}{AB(\delta_1)\Gamma(\delta_1)}\int_0^t \psi^{\delta_2-1}(t-\psi)^{\delta_1-1}\Big(W_1\big(\psi,S_n(\psi)\big)-W_1\big(\psi,S(\psi)\big)\Big)\,d\psi\Bigg\| \\
&\leq \frac{\delta_2(1-\delta_1)t^{\delta_2-1}}{AB(\delta_1)}\Big\|W_1\big(t,S_n(t)\big)-W_1\big(t,S(t)\big)\Big\| \\
&\qquad + \frac{\delta_1\delta_2}{AB(\delta_1)\Gamma(\delta_1)}\int_0^t \psi^{\delta_2-1}(t-\psi)^{\delta_1-1}\Big\|W_1\big(\psi,S_n(\psi)\big)-W_1\big(\psi,S(\psi)\big)\Big\|\,d\psi \\
&\leq \frac{\delta_2(1-\delta_1)t^{\delta_2-1}}{AB(\delta_1)}\varphi_1\Big\|S_n-S\Big\| + \frac{\delta_1\delta_2}{AB(\delta_1)\Gamma(\delta_1)}\int_0^t \psi^{\delta_2-1}(t-\psi)^{\delta_1-1}\varphi_1\Big\|S_n-S\Big\|\,d\psi \\
&\leq \left(\frac{\delta_2(1-\delta_1)}{AB(\delta_1)}+\frac{\delta_1\delta_2\Gamma(\delta_2)}{AB(\delta_1)\Gamma(\delta_1+\delta_2)}\right)\varphi_1\Big\|S_n-S\Big\| \\
&\leq \left(\frac{\delta_2(1-\delta_1)}{AB(\delta_1)}+\frac{\delta_1\delta_2\Gamma(\delta_2)}{AB(\delta_1)\Gamma(\delta_1+\delta_2)}\right)^n\kappa^n\Big\|S_1-S\Big\|.
\end{aligned}$$

It follows that $Z_{1n}(t) \Longrightarrow 0$ as $n \to \infty$ provided $\kappa < 1$.

Similarly, by taking the norm of the second function $Z_{2n}(t)$ defined above we have

$$\begin{aligned}
\left\|Z_{2n}(t)\right\| &= \left\|I_{n+1}-I\right\| \\
&= \Bigg\| \frac{\delta_2(1-\delta_1)t^{\delta_2-1}}{AB(\delta_1)}\Big(W_2\big(t,I_n(t)\big)-W_2\big(t,I(t)\big)\Big) \\
&\qquad + \frac{\delta_1\delta_2}{AB(\delta_1)\Gamma(\delta_1)}\int_0^t \psi^{\delta_2-1}(t-\psi)^{\delta_1-1}\Big(W_2\big(\psi,I_n(\psi)\big)-W_2\big(\psi,I(\psi)\big)\Big)\,d\psi\Bigg\| \\
&\leq \frac{\delta_2(1-\delta_1)t^{\delta_2-1}}{AB(\delta_1)}\Big\|W_2\big(t,I_n(t)\big)-W_2\big(t,I(t)\big)\Big\| \\
&\qquad + \frac{\delta_1\delta_2}{AB(\delta_1)\Gamma(\delta_1)}\int_0^t \psi^{\delta_2-1}(t-\psi)^{\delta_1-1}\Big\|W_2\big(\psi,I_n(\psi)\big)-W_2\big(\psi,I(\psi)\big)\Big\|\,d\psi \\
&\leq \frac{\delta_2(1-\delta_1)t^{\delta_2-1}}{AB(\delta_1)}\varphi_2\Big\|I_n-I\Big\| + \frac{\delta_1\delta_2}{AB(\delta_1)\Gamma(\delta_1)}\int_0^t \psi^{\delta_2-1}(t-\psi)^{\delta_1-1}\varphi_2\Big\|I_n-I\Big\|\,d\psi \\
&\leq \left(\frac{\delta_2(1-\delta_1)}{AB(\delta_1)}+\frac{\delta_1\delta_2\Gamma(\delta_2)}{AB(\delta_1)\Gamma(\delta_1+\delta_2)}\right)\varphi_2\Big\|I_n-I\Big\| \\
&\leq \left(\frac{\delta_2(1-\delta_1)}{AB(\delta_1)}+\frac{\delta_1\delta_2\Gamma(\delta_2)}{AB(\delta_1)\Gamma(\delta_1+\delta_2)}\right)^n\kappa^n\Big\|I_1-I\Big\|.
\end{aligned}$$

Again, it follows that $Z_{2n}(t) \Longrightarrow 0$ as $n \to \infty$ provided $\kappa < 1$. This completes the proof. □

6. Uniqueness of the Model Solutions

In this part of the study, we consider and investigate the uniqueness of the fractal-fractal model solution.

Theorem 6.1. *The non-integer deterministic Atangana-Baleanu type compartmental model (5) has a unique solution provided the inequality below holds true:*

$$\left(\frac{\delta_2(1-\delta_1)}{AB(\delta_1)} + \frac{\delta_1\delta_2\Gamma(\delta_2)}{AB(\delta_1)\Gamma(\delta_1+\delta_2)}\right)\varphi_i \leq 1, \qquad for \qquad i = 1,2. \tag{17}$$

Proof. Let us assume that there exists another solution, S̃(t), Ĩ(t) for the constructed fractal-fractional epidemiological model (5) such that

$$\begin{aligned} \tilde{S}(t) &= \frac{\delta_2(1-\delta_1)t^{\delta_2-1}}{AB(\delta_1)} W_1\left(t,\tilde{S}(t)\right) + \frac{\delta_1\delta_2}{AB(\delta_1)\Gamma(\delta_1)}\int_0^t \psi^{\delta_2-1}(t-\psi)^{\delta_1-1} W_1\left(\psi,\tilde{S}(\psi)\right)d\psi, \\ \tilde{I}(t) &= \frac{\delta_2(1-\delta_1)t^{\delta_2-1}}{AB(\delta_1)} W_2\left(t,\tilde{I}(t)\right) + \frac{\delta_1\delta_2}{AB(\delta_1)\Gamma(\delta_1)}\int_0^t \psi^{\delta_2-1}(t-\psi)^{\delta_1-1} W_2\left(\psi,\tilde{I}(\psi)\right)d\psi. \end{aligned} \tag{18}$$

Here, we take the norm of the difference between $S(t)$ and $\tilde{S}(t)$ to obtain the following results:

$$\begin{aligned} \|S(t)-\tilde{S}(t)\| &= \Bigg\| \frac{\delta_2(1-\delta_1)t^{\delta_2-1}}{AB(\delta_1)}\left(W_1\left(t,S(t)\right) - W_1\left(t,\tilde{S}(t)\right)\right) \\ &\quad + \frac{\delta_1\delta_2}{AB(\delta_1)\Gamma(\delta_1)}\int_0^t \psi^{\delta_2-1}(t-\psi)^{\delta_1-1}\left(W_1\left(\psi,S(\psi)\right) - W_1\left(\psi,\tilde{S}(\psi)\right)\right)d\psi\Bigg\| \\ &\leq \frac{\delta_2(1-\delta_1)t^{\delta_2-1}}{AB(\delta_1)}\left\|W_1\left(t,S(t)\right) - W_1\left(t,\tilde{S}(t)\right)\right\| \\ &\quad + \frac{\delta_1\delta_2}{AB(\delta_1)\Gamma(\delta_1)}\int_0^t \psi^{\delta_2-1}(t-\psi)^{\delta_1-1}\left\|W_1\left(\psi,S(\psi)\right) - W_1\left(\psi,\tilde{S}(\psi)\right)\right\|d\psi \\ &\leq \frac{\delta_2(1-\delta_1)t^{\delta_2-1}}{AB(\delta_1)}\varphi_1\left\|S-\tilde{S}\right\| + \frac{\delta_1\delta_2}{AB(\delta_1)\Gamma(\delta_1)}\int_0^t \psi^{\delta_2-1}(t-\psi)^{\delta_1-1}\varphi_1\left\|S-\tilde{S}\right\|d\psi \\ &\leq \left(\frac{\delta_2(1-\delta_1)}{AB(\delta_1)} + \frac{\delta_1\delta_2\Gamma(\delta_2)}{AB(\delta_1)\Gamma(\delta_1+\delta_2)}\right)\varphi_1\left\|S-\tilde{S}\right\|. \end{aligned}$$

We can further simplify the above inequality in the form:

$$\left[1-\left(\frac{\delta_2(1-\delta_1)}{AB(\delta_1)}+\frac{\delta_1\delta_2\Gamma(\delta_2)}{AB(\delta_1)\Gamma(\delta_1+\delta_2)}\right)\varphi_1\right]\left\|S-\tilde{S}\right\|\leq 0.$$

From this inequality we can write that $\left\|S-\tilde{S}\right\|=0$. It then follows that $S=\tilde{S}$.

$$\begin{aligned}\|I(t)-\tilde{I}(t)\| &= \Bigg\|\frac{\delta_2(1-\delta_1)t^{\delta_2-1}}{AB(\delta_1)}\Big(W_2\big(t,I(t)\big)-W_2\big(t,\tilde{I}(t)\big)\Big)\\ &\quad+\frac{\delta_1\delta_2}{AB(\delta_1)\Gamma(\delta_1)}\int_0^t\psi^{\delta_2-1}(t-\psi)^{\delta_1-1}\Big(W_2\big(\psi,I(\psi)\big)-W_2\big(\psi,\tilde{I}(\psi)\big)\Big)\,d\psi\Bigg\|\\ &\leq\frac{\delta_2(1-\delta_1)t^{\delta_2-1}}{AB(\delta_1)}\left\|W_2\big(t,I(t)\big)-W_2\big(t,\tilde{I}(t)\big)\right\|\\ &\quad+\frac{\delta_1\delta_2}{AB(\delta_1)\Gamma(\delta_1)}\int_0^t\psi^{\delta_2-1}(t-\psi)^{\delta_1-1}\left\|W_2\big(\psi,I(\psi)\big)-W_2\big(\psi,\tilde{I}(\psi)\big)\right\|d\psi\\ &\leq\frac{\delta_2(1-\delta_1)t^{\delta_2-1}}{AB(\delta_1)}\varphi_2\left\|I-\tilde{I}\right\|+\frac{\delta_1\delta_2}{AB(\delta_1)\Gamma(\delta_1)}\int_0^t\psi^{\delta_2-1}(t-\psi)^{\delta_1-1}\varphi_2\left\|I-\tilde{I}\right\|d\psi\\ &\leq\left(\frac{\delta_2(1-\delta_1)}{AB(\delta_1)}+\frac{\delta_1\delta_2\Gamma(\delta_2)}{AB(\delta_1)\Gamma(\delta_1+\delta_2)}\right)\varphi_2\left\|I-\tilde{I}\right\|.\end{aligned}$$

Further simplification of the above inequality gives

$$\left[1-\left(\frac{\delta_2(1-\delta_1)}{AB(\delta_1)}+\frac{\delta_1\delta_2\Gamma(\delta_2)}{AB(\delta_1)\Gamma(\delta_1+\delta_2)}\right)\varphi_2\right]\left\|I-\tilde{I}\right\|\leq 0.$$

From this inequality we can state that $\left\|I-\tilde{I}\right\|=0$. It then follows that $I=\tilde{I}$. This completes the proof. □

7. Hyers-Ulam Stability

Definition 7.1. The integral system (13) is said to be Hyers-Ulam stable if there exist a constant $v_i>0$ for $i\in N_1{}^2$, satisfying for every $\vartheta_i,\ i\in N_1{}^2$.

$$\left|S(t)-\frac{\delta_2(1-\delta_1)t^{\delta_2-1}}{AB(\delta_1)}W_1\big(t,S(t)\big)-\frac{\delta_1\delta_2}{AB(\delta_1)\Gamma(\delta_1)}\int_0^t\psi^{\delta_2-1}(t-\psi)^{\delta_1-1}W_1\big(\psi,S(\psi)\big)\,d\psi\right|\leq\vartheta_1,$$

$$\left|I(t)-\frac{\delta_2(1-\delta_1)t^{\delta_2-1}}{AB(\delta_1)}W_2\big(t,I(t)\big)-\frac{\delta_1\delta_2}{AB(\delta_1)\Gamma(\delta_1)}\int_0^t\psi^{\delta_2-1}(t-\psi)^{\delta_1-1}W_2\big(\psi,I(\psi)\big)\,d\psi\right|\leq\vartheta_2.$$

There exist approximate solution $(S^{\maltese}(t), I^{\maltese}(t))$ for the model problem (5) satisfying the following integral equations

$$S^{\maltese}(t) = \frac{\delta_2(1-\delta_1)t^{\delta_2-1}}{AB(\delta_1)} W_1\Big(t, S^{\maltese}(t)\Big) + \frac{\delta_1\delta_2}{AB(\delta_1)\Gamma(\delta_1)} \int_0^t \psi^{\delta_2-1}(t-\psi)^{\delta_1-1} W_1\Big(\psi, S^{\maltese}(\psi)\Big)\, d\psi,$$

$$I^{\maltese}(t) = \frac{\delta_2(1-\delta_1)t^{\delta_2-1}}{AB(\delta_1)} W_2\Big(t, I^{\maltese}(t)\Big) + \frac{\delta_1\delta_2}{AB(\delta_1)\Gamma(\delta_1)} \int_0^t \psi^{\delta_2-1}(t-\psi)^{\delta_1-1} W_2\Big(\psi, I^{\maltese}(\psi)\Big)\, d\psi.$$

such that

$$\Big|S(t) - S^{\maltese}(t)\Big| \leq \tau_1 \vartheta_1,$$
$$\Big|I(t) - I^{\maltese}(t)\Big| \leq \tau_1 \vartheta_2.$$

Theorem 7.1. *Suppose that assumption (Q^*) is satisfied then the model problem (5) is Hyers-Ulam stable.*

Proof. Following the results from theorem (6.1), we have established that the nonlinear deterministic model (5) has a unique solution. Let consider $(S^{\maltese}(t), I^{\maltese}(t))$ to be the approximate solution of the mathematical model, then we have

$$\begin{aligned}
\Big|S(t) - S^{\maltese}(t)\Big| &= \Bigg|\frac{\delta_2(1-\delta_1)t^{\delta_2-1}}{AB(\delta_1)}\Big(W_1\Big(t, S(t)\Big) - W_1\Big(t, S^{\maltese}(t)\Big)\Big) \\
&\quad + \frac{\delta_1\delta_2}{AB(\delta_1)\Gamma(\delta_1)} \int_0^t \psi^{\delta_2-1}(t-\psi)^{\delta_1-1}\Big(W_1\Big(\psi, S(\psi)\Big) - W_1\Big(\psi, S^{\maltese}(\psi)\Big)\Big)\, d\psi\Bigg| \\
&\leq \frac{\delta_2(1-\delta_1)t^{\delta_2-1}}{AB(\delta_1)} \varphi_1 \Big\|S - S^{\maltese}\Big\| + \frac{\delta_1\delta_2}{AB(\delta_1)\Gamma(\delta_1)} \int_0^t \psi^{\delta_2-1}(t-\psi)^{\delta_1-1} \varphi_1 \Big\|S - S^{\maltese}\Big\|\, d\psi \\
&\leq \left(\frac{\delta_2(1-\delta_1)}{AB(\delta_1)} + \frac{\delta_1\delta_2\Gamma(\delta_2)}{AB(\delta_1)\Gamma(\delta_1+\delta_2)}\right) \varphi_1 \Big\|S - S^{\maltese}\Big\|.
\end{aligned}$$

Now, let $\varphi_1 = \vartheta_1$, $\left(\frac{\delta_2(1-\delta_1)}{AB(\delta_1)} + \frac{\delta_1\delta_2\Gamma(\delta_2)}{AB(\delta_1)\Gamma(\delta_1+\delta_2)}\right)\Big\|S - S^{\maltese}\Big\| = \nu_1$. Then we have

$$\Big|S(t) - S^{\maltese}(t)\Big| \leq \nu_1 \vartheta_1.$$

$$\begin{aligned}\left|I(t)-I^{\maltese}(t)\right| = & \left|\frac{\delta_2(1-\delta_1)t^{\delta_2-1}}{AB(\delta_1)}\left(W_2\left(t,I(t)\right)-W_2\left(t,I^{\maltese}(t)\right)\right)\right. \\ & \left.+\frac{\delta_1\delta_2}{AB(\delta_1)\Gamma(\delta_1)}\int_0^t \psi^{\delta_2-1}(t-\psi)^{\delta_1-1}\left(W_2\left(\psi,I(\psi)\right)-W_2\left(\psi,I^{\maltese}(\psi)\right)\right)d\psi\right| \\ \leq & \frac{\delta_2(1-\delta_1)t^{\delta_2-1}}{AB(\delta_1)}\varphi_2\left\|I-I^{\maltese}\right\|+\frac{\delta_1\delta_2}{AB(\delta_1)\Gamma(\delta_1)}\int_0^t \psi^{\delta_2-1}(t-\psi)^{\delta_1-1}\varphi_2\left\|I-I^{\maltese}\right\|d\psi \\ \leq & \left(\frac{\delta_2(1-\delta_1)}{AB(\delta_1)}+\frac{\delta_1\delta_2\Gamma(\delta_2)}{AB(\delta_1)\Gamma(\delta_1+\delta_2)}\right)\varphi_2\left\|I-I^{\maltese}\right\|.\end{aligned}$$

Similarly, let $\varphi_2 = \vartheta_2$, $\left(\frac{\delta_2(1-\delta_1)}{AB(\delta_1)}+\frac{\delta_1\delta_2\Gamma(\delta_2)}{AB(\delta_1)\Gamma(\delta_1+\delta_2)}\right)\left\|I-I^{\maltese}\right\| = \nu_2$. Then the above inequality takes the form given below:

$$\left|I(t)-I^{\maltese}(t)\right| \leq \nu_2\vartheta_2.$$

Hence the results follows. □

8. ITERATIVE SCHEME FOR FRACTAL-FRACTIONAL MODEL PROBLEM

In this section, we will provide a brief construction of the numerical iterative scheme that we will use to solve our model problem in this study. The detailed analytical construction of this novel Newton polynomial based iterative scheme for fractal-fractional model problems characterized by the Atangana-Baleanu derivative can be found in a numerical computational textbook written by Atangana and Araz [60]. It is important to mention that this newly developed iterative scheme has been applied in some recent works by the authors in [61, 62, 57, 63] to numerically solve their mathematical models.

Let us consider a fractal-fractional initial value problem given by

$$\begin{cases} {}_0^{FF}D_t^{\delta_1,\delta_2}p(t) = \xi\left(t,p(t)\right), \\ p(0) = p_0. \end{cases} \tag{19}$$

Then by using the fractal-fractional integral, we convert equation (19) into

$$p(t)-p(0) = \frac{\delta_2(1-\delta_1)t^{\delta_2-1}}{AB(\delta_1)}\xi\left(t,p(t)\right)+\frac{\delta_1\delta_2}{AB(\delta_1)\Gamma(\delta_1)}\int_0^t \psi^{\delta_2-1}\xi\left(\psi,p(\psi)\right)(t-\psi)^{\delta_1-1}d\psi. \tag{20}$$

Let $Q\Big(t,p(t)\Big)=\delta_2 t^{\delta_2-1}\xi\Big(t,p(t)\Big)$. Therefore at the point $t_{m+1}=(m+1)h$, we obtain

$$p(t_{m+1})-p(0)=\frac{(1-\delta_1)}{AB(\delta_1)}Q\Big(t_m,p(t_m)\Big)+\frac{\delta_1}{AB(\delta_1)\Gamma(\delta_1)}\int_0^{t_{m+1}}Q\Big(\psi,p(\psi)\Big)(t_{m+1}-\psi)^{\delta_1-1}d\psi. \tag{21}$$

Next, by applying Newton polynomial and performing some detailed analytical calculations and simplifications, the iterative scheme for the fractal-fractional model problem (19) is given by

$$\begin{aligned}
p^{m+1} =& p_0+\frac{(1-\delta_1)}{AB(\delta_1)}\delta_2 t_m^{\delta_2-1}\xi\Big(t_m,p^m\Big)\\
&+\frac{\delta_1 h^{\delta_1}}{AB(\delta_1)\Gamma(\delta_1+1)}\sum_{\vartheta=2}^{m}\delta_2 t_{\vartheta-2}^{\delta_2-1}\xi\Big(t_{\vartheta-2},p^{\vartheta-2}\Big)\Big[\Big(m-\vartheta+1\Big)^{\delta_1}-\Big(m-\vartheta\Big)^{\delta_1}\Big]\\
&+\frac{\delta_1 h^{\delta_1}}{AB(\delta_1)\Gamma(\delta_1+2)}\sum_{\vartheta=2}^{m}\begin{bmatrix}\delta_2 t_{\vartheta-1}^{\delta_2-1}\xi\Big(t_{\vartheta-1},p^{\vartheta-1}\Big)\\ \delta_2 t_{\vartheta-2}^{\delta_2-1}\xi\Big(t_{\vartheta-2},p^{\vartheta-2}\Big)\end{bmatrix}\times\begin{bmatrix}\Big(m-\vartheta+1\Big)^{\delta_1}\Big(m-\vartheta+3+2\delta_1\Big)\\ -\Big(m-\vartheta\Big)^{\delta_1}\Big(m-\vartheta+3+3\delta_1\Big)\end{bmatrix}\\
&+\frac{\delta_1 h^{\delta_1}}{2AB(\delta_1)\Gamma(\delta_1+3)}\sum_{\vartheta=2}^{m}\begin{bmatrix}\delta_2 t_{\vartheta}^{\delta_2-1}\xi\Big(t_{\vartheta},p^{\vartheta}\Big)\\ -2\delta_2 t_{\vartheta-1}^{\delta_2-1}\xi\Big(t_{\vartheta-1},p^{\vartheta-1}\Big)\\ +\delta_2 t_{\vartheta-2}^{\delta_2-1}\xi\Big(t_{\vartheta-2},p^{\vartheta-2}\Big)\end{bmatrix}\\
&\times\begin{bmatrix}\Big(m-\vartheta+1\Big)^{\delta_1}\Big[2\Big(m-\vartheta\Big)^2+\Big(3\delta_1-10\Big)\Big(m-\vartheta\Big)+2\delta_1^2+9\delta_1+12\Big]\\ -\Big(m-\vartheta\Big)^{\delta_1}\Big[2\Big(m-\vartheta\Big)^2+\Big(5\delta_1-10\Big)\Big(m-\vartheta\Big)+6\delta_1^2+18\delta_1+12\Big]\end{bmatrix}.
\end{aligned} \tag{22}$$

Converting the nonlinear fractal-fractional SIRS epidemic model (5) into the form of the initial value problem (19) we have

$$\begin{cases}{}_0^{FF}D_t^{\delta_1,\delta_2}S(t)=H_1\Big(t,S(t),I(t)\Big),\\ {}_0^{FF}D_t^{\delta_1,\delta_2}I(t)=H_2\Big(t,S(t),I(t)\Big),\\ S(0)=S_0;\ I(0)=I_0.\end{cases} \tag{23}$$

Following the iterative scheme given by equation (22), the corresponding Newton polynomial based iterative scheme for our model problem (23) can be written as follows:

$$
\begin{aligned}
S^{m+1} =& S_0 + \frac{(1-\delta_1)}{AB(\delta_1)}\delta_2 t_m^{\delta_2-1} H_1\left(t_m, S^m, I^m\right) \\
&+ \frac{\delta_1 h^{\delta_1}}{AB(\delta_1)\Gamma(\delta_1+1)} \sum_{\vartheta=2}^{m} \delta_2 t_{\vartheta-2}^{\delta_2-1} H_1\left(t_{\vartheta-2}, S^{\vartheta-2}, I^{\vartheta-2}\right)\left[\left(m-\vartheta+1\right)^{\delta_1} - \left(m-\vartheta\right)^{\delta_1}\right] \\
&+ \frac{\delta_1 h^{\delta_1}}{AB(\delta_1)\Gamma(\delta_1+2)} \sum_{\vartheta=2}^{m} \begin{bmatrix} \delta_2 t_{\vartheta-1}^{\delta_2-1} H_1\left(t_{\vartheta-1}, S^{\vartheta-1}, I^{\vartheta-1}\right) \\ \delta_2 t_{\vartheta-2}^{\delta_2-1} H_1\left(t_{\vartheta-2}, S^{\vartheta-2}, I^{\vartheta-2}\right) \end{bmatrix} \times \begin{bmatrix} \left(m-\vartheta+1\right)^{\delta_1}\left(m-\vartheta+3+2\delta_1\right) \\ -\left(m-\vartheta\right)^{\delta_1}\left(m-\vartheta+3+3\delta_1\right) \end{bmatrix} \\
&+ \frac{\delta_1 h^{\delta_1}}{2AB(\delta_1)\Gamma(\delta_1+3)} \sum_{\vartheta=2}^{m} \begin{bmatrix} \delta_2 t_{\vartheta}^{\delta_2-1} H_1\left(t_{\vartheta}, S^{\vartheta}, I^{\vartheta}\right) \\ -2\delta_2 t_{\vartheta-1}^{\delta_2-1} H_1\left(t_{\vartheta-1}, S^{\vartheta-1}, I^{\vartheta-1}\right) \\ +\delta_2 t_{\vartheta-2}^{\delta_2-1} H_1\left(t_{\vartheta-2}, S^{\vartheta-2}, I^{\vartheta-2}\right) \end{bmatrix} \\
&\times \begin{bmatrix} \left(m-\vartheta+1\right)^{\delta_1}\left[2\left(m-\vartheta\right)^2 + \left(3\delta_1-10\right)\left(m-\vartheta\right) + 2\delta_1^2 + 9\delta_1 + 12\right] \\ -\left(m-\vartheta\right)^{\delta_1}\left[2\left(m-\vartheta\right)^2 + \left(5\delta_1-10\right)\left(m-\vartheta\right) + 6\delta_1^2 + 18\delta_1 + 12\right] \end{bmatrix}.
\end{aligned} \tag{24}
$$

$$
\begin{aligned}
I^{m+1} =& I_0 + \frac{(1-\delta_1)}{AB(\delta_1)}\delta_2 t_m^{\delta_2-1} H_2\left(t_m, S^m, I^m,\right) \\
&+ \frac{\delta_1 h^{\delta_1}}{AB(\delta_1)\Gamma(\delta_1+1)} \sum_{\vartheta=2}^{m} \delta_2 t_{\vartheta-2}^{\delta_2-1} H_2\left(t_{\vartheta-2}, S^{\vartheta-2}, I^{\vartheta-2}\right)\left[\left(m-\vartheta+1\right)^{\delta_1} - \left(m-\vartheta\right)^{\delta_1}\right] \\
&+ \frac{\delta_1 h^{\delta_1}}{AB(\delta_1)\Gamma(\delta_1+2)} \sum_{\vartheta=2}^{m} \begin{bmatrix} \delta_2 t_{\vartheta-1}^{\delta_2-1} H_2\left(t_{\vartheta-1}, S^{\vartheta-1}, I^{\vartheta-1}\right) \\ \delta_2 t_{\vartheta-2}^{\delta_2-1} H_2\left(t_{\vartheta-2}, S^{\vartheta-2}, I^{\vartheta-2}\right) \end{bmatrix} \times \begin{bmatrix} \left(m-\vartheta+1\right)^{\delta_1}\left(m-\vartheta+3+2\delta_1\right) \\ -\left(m-\vartheta\right)^{\delta_1}\left(m-\vartheta+3+3\delta_1\right) \end{bmatrix} \\
&+ \frac{\delta_1 h^{\delta_1}}{2AB(\delta_1)\Gamma(\delta_1+3)} \sum_{\vartheta=2}^{m} \begin{bmatrix} \delta_2 t_{\vartheta}^{\delta_2-1} H_2\left(t_{\vartheta}, S^{\vartheta}, I^{\vartheta}\right) \\ -2\delta_2 t_{\vartheta-1}^{\delta_2-1} H_2\left(t_{\vartheta-1}, S^{\vartheta-1}, I^{\vartheta-1}\right) \\ +\delta_2 t_{\vartheta-2}^{\delta_2-1} H_2\left(t_{\vartheta-2}, S^{\vartheta-2}, I^{\vartheta-2}\right) \end{bmatrix} \\
&\times \begin{bmatrix} \left(m-\vartheta+1\right)^{\delta_1}\left[2\left(m-\vartheta\right)^2 + \left(3\delta_1-10\right)\left(m-\vartheta\right) + 2\delta_1^2 + 9\delta_1 + 12\right] \\ -\left(m-\vartheta\right)^{\delta_1}\left[2\left(m-\vartheta\right)^2 + \left(5\delta_1-10\right)\left(m-\vartheta\right) + 6\delta_1^2 + 18\delta_1 + 12\right] \end{bmatrix}.
\end{aligned} \tag{25}
$$

8.1. Simulation Results and Discussion. This subsection of our study is concerned with the numerical results, which include both solution paths and phase portraits of the fractal-fractional model. The nonlinear deterministic model is simulated using the Newton polynomial-based numerical iterative scheme [60] briefly presented in the previous section. For this purpose, the numerical solutions or trajectories of the newly constructed fractal-fractional model (5) were obtained by utilizing the following initial conditions: $S(0) = 0.99$ and $I(0) = 0.01$. Additionally, the following parameter values were also utilized, where $\rho = \frac{1}{65*365}$, $\eta = 0.02$, $\gamma = \frac{1}{3}$, and $\beta = \mathscr{R}_0 * (\gamma + \rho)$ with $\mathscr{R}_0 = 3$. Furthermore, in these numerical illustrations, it is important to note that the same parameter values were used to generate the various numerical solutions and phase portraits except in Figure 6, where $\beta = \mathscr{R}_0 * (\gamma + \rho)$ with $\mathscr{R}_0 = 0.8$ was utilized. Figures 2(a) and 2(b) show the fractal dynamics of the proposed model. It is noticed in Figure 2(a) that the fractal order of 0.99 takes the same trajectory shape as the fractional order of 1 and increases above the other fractal orders. In Figure 2(b), it can be seen that the trajectory shapes of the various fractal orders are the same, but there is a shift in the epidemic peak as the fractal order reduces. This indicates that, during an epidemic spread, the behavioural nature of individuals affects the epidemic, resulting in a delay of the epidemic peak. Figures 2(c) and 2(d) show the fractional dynamics of the proposed model. It is noticed in Figure 2(c) that the fractional order takes the same trajectory shape as the integer order of 1 and increases as the fractional order decreases. In Figure 2(d), it can be observed that the trajectory shapes of the various fractional orders are the same, but there is a reduction in the epidemic peak as the fractional order reduces. Figures 2(e) and 2(f) show the fractal-fractional dynamics of the proposed model. It is noticed in Figure 2(e) that the fractal-fractional nature of susceptible increases as the fractal-fractional order reduces. In Figure 2(f), it can be seen that the trajectory shapes of the various fractal-fractional orders give a unique curve, where the epidemic peaks are below the preceding fractal-fractional orders. The trajectories in Figures 2(a)-2(f) show the hidden inner dynamics of the model and the memory effects on each compartmental class. Furthermore, Figures 3-6 show that there are inter-unique phase portraits for the fractal-fractional epidemic model when the fractal-fractional order is changed.

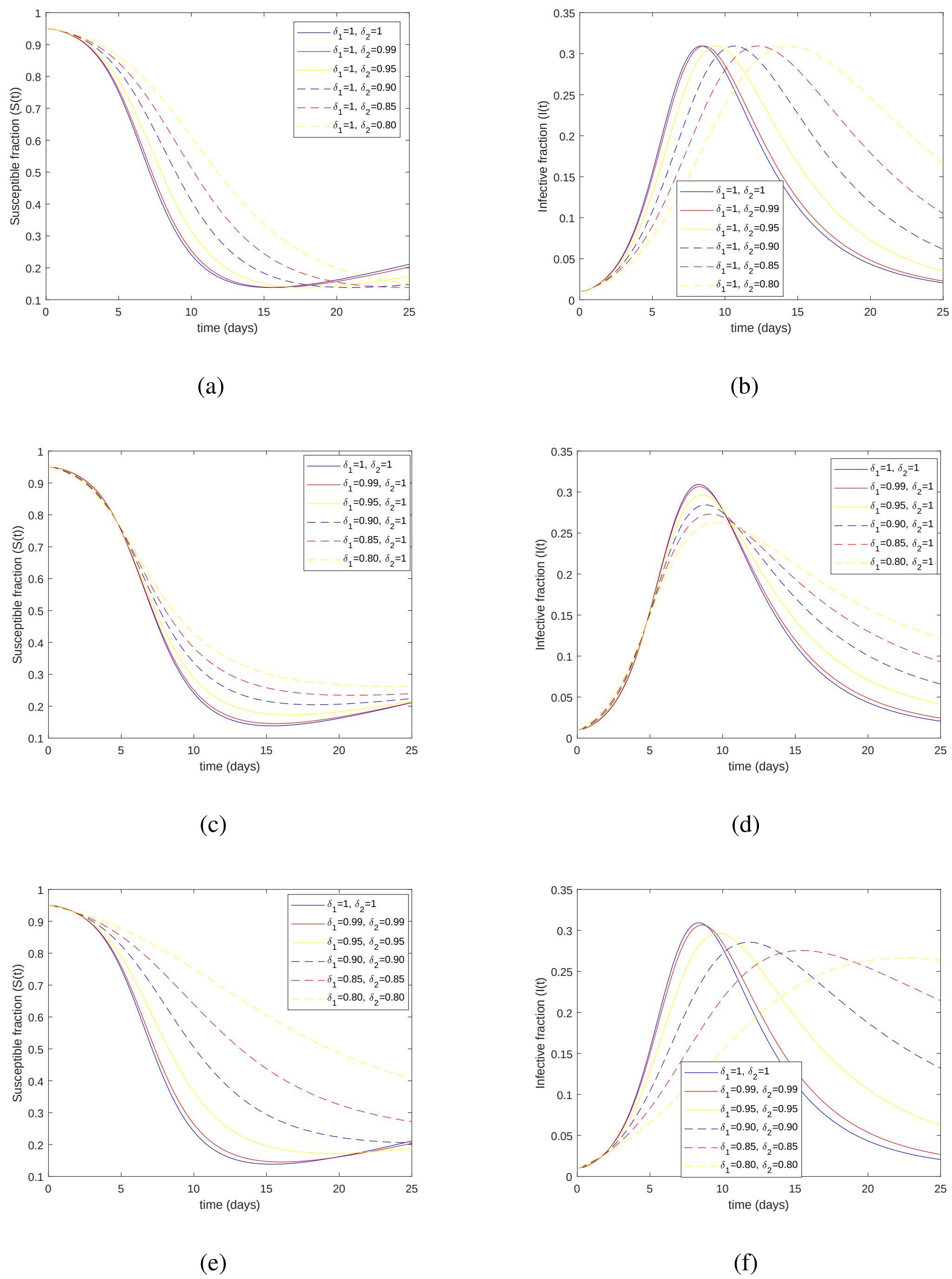

FIGURE 2. Solution paths for the fractal-fractional epidemic model for different selected values of $\delta_1(1,0.99,0.95,0.90,0.85,0.80)$ and $\delta_2(1,0.99,0.95,0.90,0.85,0.80)$ as shown in the various subplots with $\mathscr{R}_0 = 3$.

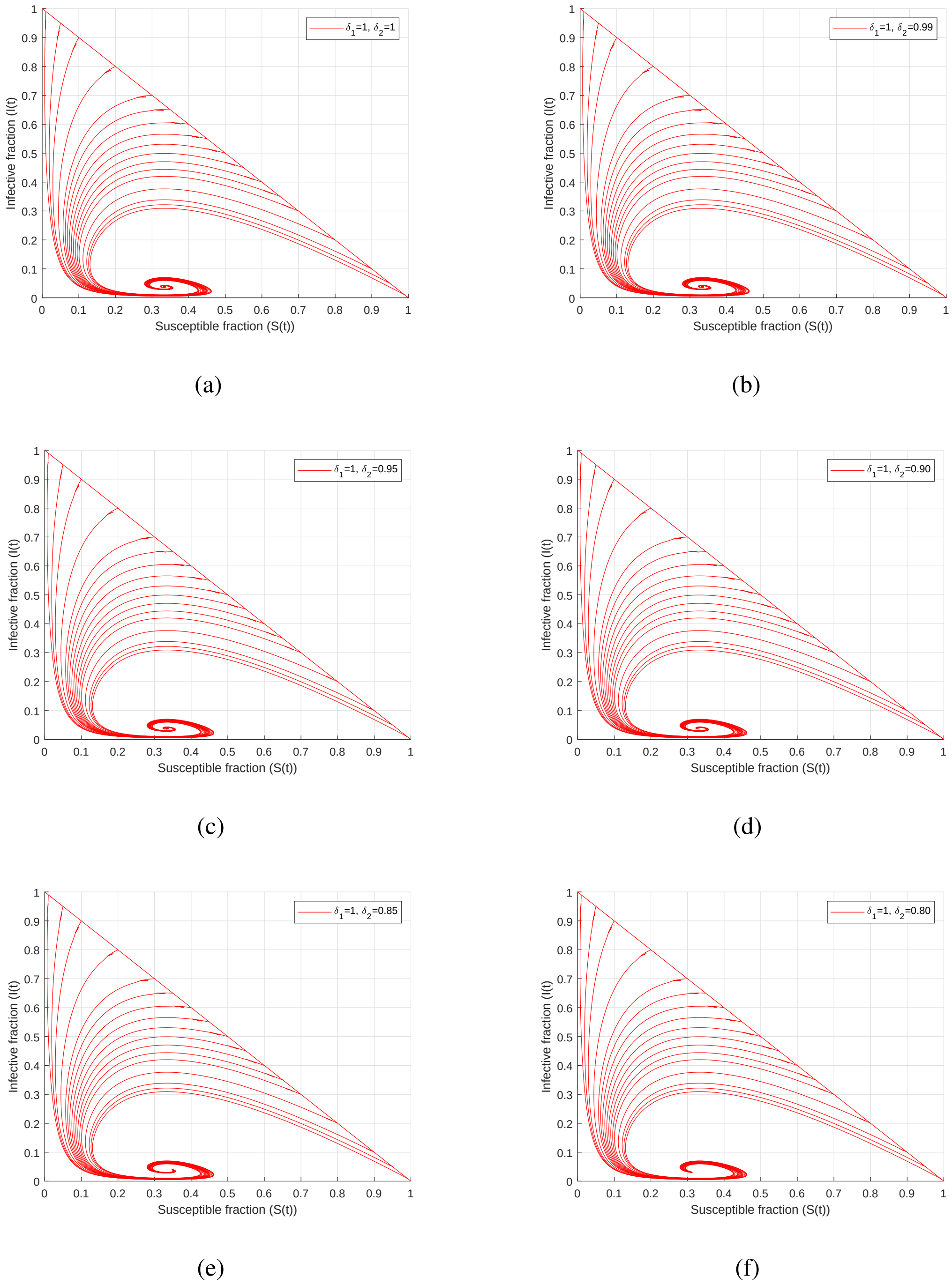

FIGURE 3. Phase portraits for the fractal-fractional epidemic model for $\delta_2 = 1, 0.99, 0.95, 0.90, 0.85, 0.80$ with fixed $\delta_1 = 1$ and $\mathscr{R}_0 = 3$.

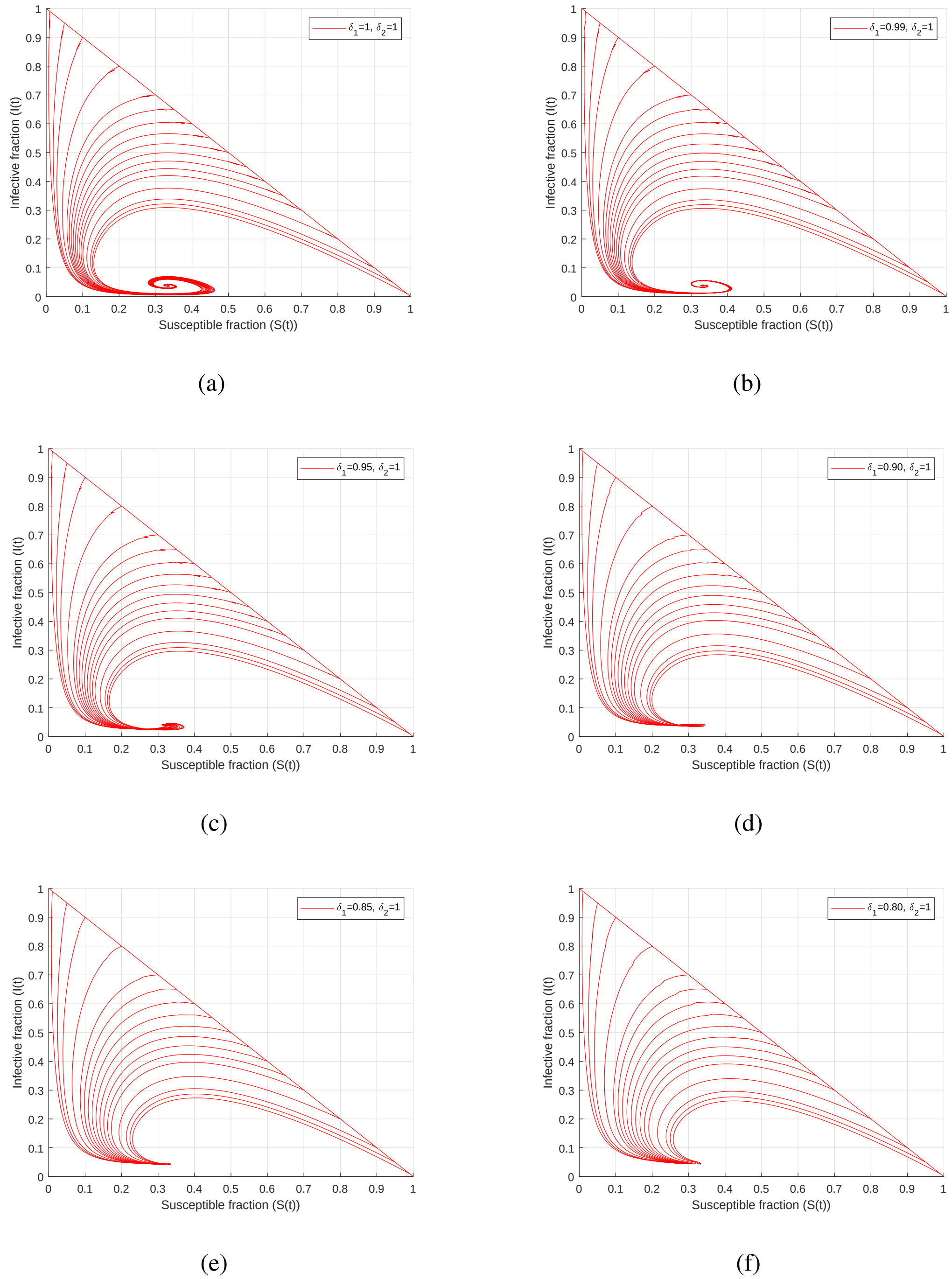

FIGURE 4. Phase portraits for the fractal-fractional epidemic model for $\delta_1 = 1, 0.99, 0.95, 0.90, 0.85, 0.80$ with fixed $\delta_2 = 1$ and $\mathscr{R}_0 = 3$.

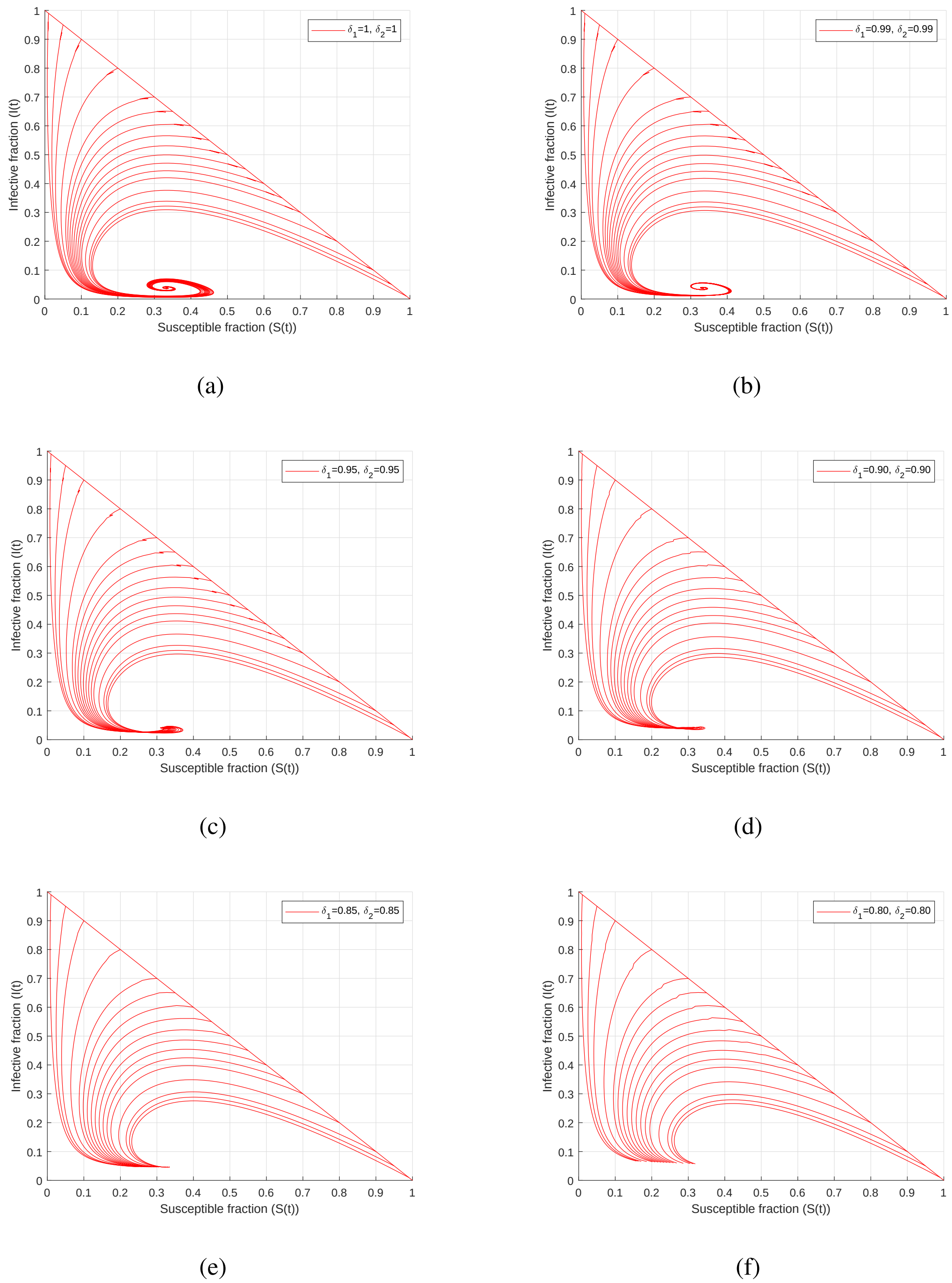

FIGURE 5. Phase portraits for the fractal-fractional epidemic model with $\delta_1 = \delta_2 = 1, 0.99, 0.95, 0.90, 0.85, 0.80$ and $\mathscr{R}_0 = 3$.

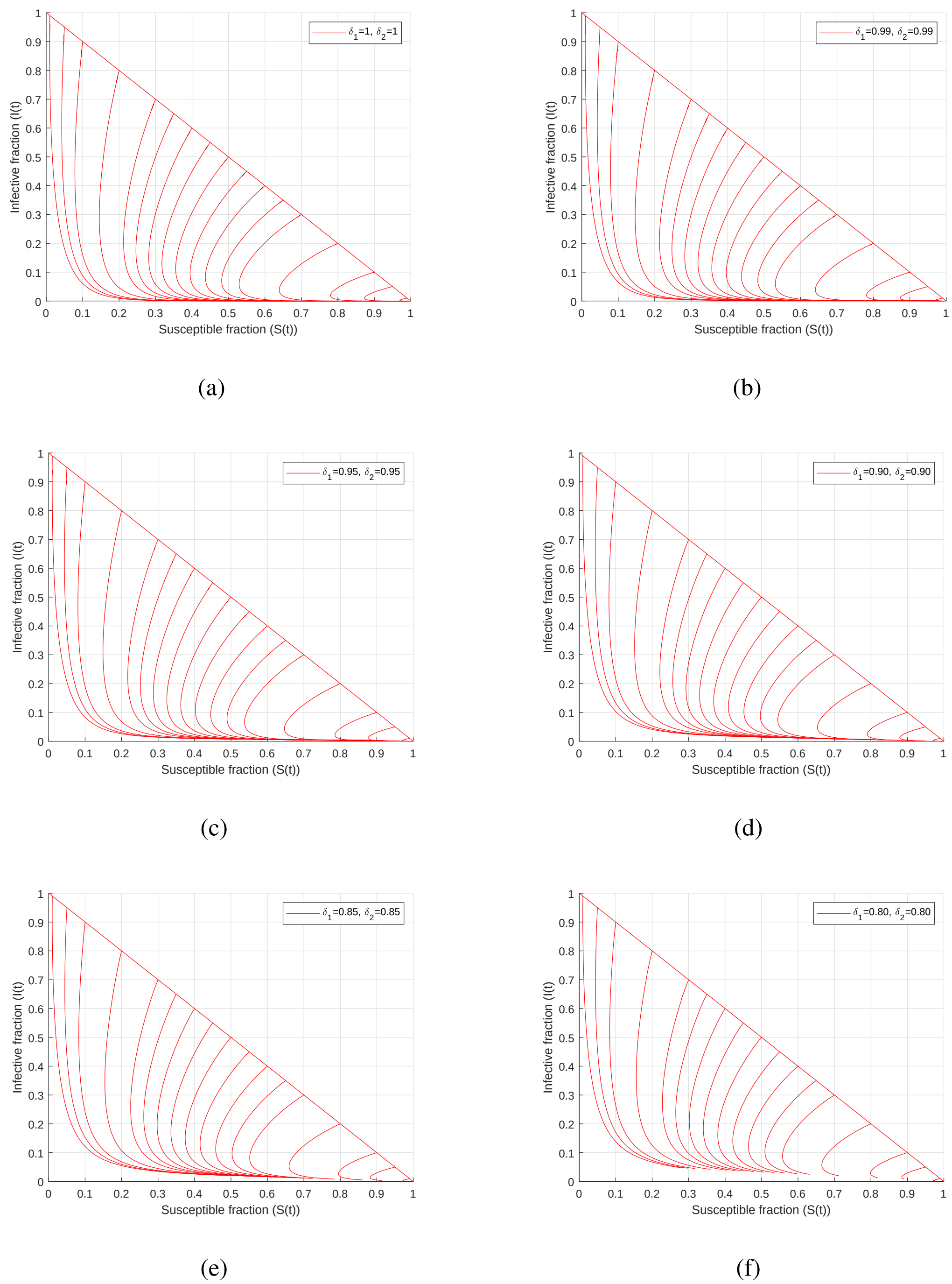

FIGURE 6. Phase portraits for the fractal-fractional epidemic model with $\delta_1 = \delta_2 = 1, 0.99, 0.95, 0.90, 0.85, 0.80$ and $\mathscr{R}_0 = 0.8$.

9. Conclusion

In our present mathematical modeling formulation, we have proposed and studied a nonlinear Atangana-Baleanu fractal-fractional SIRS deterministic model. The model's equilibrium points (disease-free and endemic) are studied for local asymptotic stability. The existence of the model's solution and its uniqueness, as well as the Hyers-Ulam stability analysis, are established. The recently developed and effective Newton polynomial-based iterative scheme for nonlinear fractal-fractional model problems has been used to solve our proposed SIRS deterministic model. Our numerical solution shows that there is a shift in the epidemic peak when we fix the fractional order and vary the fractal order. Also, when the fractal order is fixed but the fractional order varies, the epidemic peak shifts and reduces. Additionally, when both the fractal and fractional orders are simultaneously varied, we notice a shift and reduction in the epidemic peak. These dynamics show that when an epidemic spreads, the behavior of the people affects the epidemic, thus causing it to take a longer time to reach its peak. Additionally, for different selected values of the fractal and fractional orders, phase portraits for the newly constructed model are also generated. Our numerical simulations demonstrate that fractal-fractional dynamic modeling is a very useful and appropriate mathematical modeling tool for developing and studying epidemiological models.

Disclosure Statement

The authors fully acknowledge that this paper was developed from the results of the first author's ongoing Ph.D. research in the Department of Mathematics, School of Mathematical Sciences at the C. K. Tedam University of Technology and Applied Sciences, Navrongo, Ghana.

CRediT Authorship Contribution Statement

E. Okyere: Conceptualization, Methodology, Formal analysis, Investigation, Writing-original draft, Review & editing.

B. Seidu: Supervision, Methodology, Writing - review & editing.

K. Nantomah: Supervision, Methodology, Writing - review & editing.

J. K. K. Asamoah: Writing-review & editing.

Conflict of Interests

The authors declare that there is no conflict of interests.

References

[1] H.W. Hethcote, The mathematics of infectious diseases, SIAM Rev. 42 (2000), 599-653. https://doi.org/10.1137/s0036144500371907.

[2] B. Seidu, O.D. Makinde, Optimal control of HIV/AIDS in the workplace in the presence of careless individuals, Comput. Math. Methods Med. 2014 (2014), 831506. https://doi.org/10.1155/2014/831506.

[3] J.M. Trauer, J.T. Denholm, E.S. McBryde, Construction of a mathematical model for tuberculosis transmission in highly endemic regions of the Asia-pacific, J. Theor. Biol. 358 (2014), 74–84. https://doi.org/10.1016/j.jtbi.2014.05.023.

[4] B. Seidu, C.S. Bornaa, O.D. Makinde, An Ebola model with hyper-susceptibility, Chaos Solitons Fractals. 138 (2020), 109938. https://doi.org/10.1016/j.chaos.2020.109938.

[5] R. Kicsiny, J. Nagy, Cs. Szalóki, Extended ordinary differential equation models for solar heating systems with pipes, Appl. Energy. 129 (2014), 166–176. https://doi.org/10.1016/j.apenergy.2014.04.108.

[6] J.K.K. Asamoah, M.A. Owusu, Z. Jin, et al. Global stability and cost-effectiveness analysis of COVID-19 considering the impact of the environment: using data from Ghana, Chaos Solitons Fractals. 140 (2020), 110103. https://doi.org/10.1016/j.chaos.2020.110103.

[7] C.J. Silva, D.F.M. Torres, A SICA compartmental model in epidemiology with application to HIV/AIDS in Cape Verde, Ecol. Complex. 30 (2017), 70–75. https://doi.org/10.1016/j.ecocom.2016.12.001.

[8] J.K.K. Asamoah, Z. Jin, G.-Q. Sun, et al. Sensitivity assessment and optimal economic evaluation of a new COVID-19 compartmental epidemic model with control interventions, Chaos Solitons Fractals. 146 (2021), 110885. https://doi.org/10.1016/j.chaos.2021.110885.

[9] A.B. Hogan, K. Glass, H.C. Moore, R.S. Anderssen, Age structures in mathematical models for infectious diseases, with a case study of respiratory syncytial virus, in: R.S. Anderssen, P. Broadbridge, Y. Fukumoto, K. Kajiwara, T. Takagi, E. Verbitskiy, M. Wakayama (Eds.), Applications + Practical Conceptualization + Mathematics = Fruitful Innovation, Springer Japan, Tokyo, 2016: pp. 105–116. https://doi.org/10.1007/978-4-431-55342-7_9.

[10] G. Yakubu, P. Olejnik, J. Awrejcewicz, On the modeling and simulation of variable-length pendulum systems: A review, Arch. Comput. Methods Eng. 29 (2022), 2397–2415. https://doi.org/10.1007/s11831-021-09658-8.

[11] T.F. Reid, S.C. King, Pendulum motion and differential equations, Probl. Resources Iss. Math. Undergrad. Stud. (PRIMUS). 19 (2009), 205–217. https://doi.org/10.1080/10511970701693942.

[12] A. ul Rehman, R. Singh, T. Abdeljawad, E. Okyere, L. Guran, Modeling, analysis and numerical solution to malaria fractional model with temporary immunity and relapse, Adv. Differ. Equ. 2021 (2021), 390. https://doi.org/10.1186/s13662-021-03532-4.

[13] I. Podlubny, Fractional differential equations: An introduction to fractional derivatives, fractional differential equations, to methods of their solution and some of their applications, Academic Press, San Diego, 1999. https://www.sciencedirect.com/bookseries/mathematics-in-science-and-engineering/vol/198/suppl/C.

[14] W.E. Raslan, Fractional mathematical modeling for epidemic prediction of COVID-19 in Egypt, Ain Shams Eng. J. 12 (2021), 3057–3062. https://doi.org/10.1016/j.asej.2020.10.027.

[15] I. Petras, Novel fractional-order model predictive control: State-space approach, IEEE Access. 9 (2021), 92769–92775. https://doi.org/10.1109/access.2021.3093364.

[16] C.M.A. Pinto, A.R.M. Carvalho, A latency fractional order model for HIV dynamics, J. Comput. Appl. Math. 312 (2017), 240–256. https://doi.org/10.1016/j.cam.2016.05.019.

[17] A. Carvalho, C.M.A. Pinto, A delay fractional order model for the co-infection of malaria and HIV/AIDS, Int. J. Dynam. Control. 5 (2016), 168–186. https://doi.org/10.1007/s40435-016-0224-3.

[18] A.R. Carvalho, C.M. Pinto, D. Baleanu, HIV/HCV coinfection model: a fractional-order perspective for the effect of the HIV viral load, Adv. Differ. Equ. 2018 (2018), 2. https://doi.org/10.1186/s13662-017-1456-z.

[19] D. Kumar, J. Singh, M. Al Qurashi, D. Baleanu, A new fractional SIRS-SI malaria disease model with application of vaccines, antimalarial drugs, and spraying, Adv. Differ. Equ. 2019 (2019), 278. https://doi.org/10.1186/s13662-019-2199-9.

[20] S. Ullah, M. Altaf Khan, M. Farooq, A fractional model for the dynamics of TB virus, Chaos Solitons Fractals. 116 (2018), 63–71. https://doi.org/10.1016/j.chaos.2018.09.001.

[21] D. Baleanu, Z.B. Guvenc, J.A.T. Machado, eds., New trends in nanotechnology and fractional calculus applications, Springer Netherlands, Dordrecht, 2010. https://doi.org/10.1007/978-90-481-3293-5.

[22] Y. Qiao, H. Xu, H. Qi, Numerical simulation of a two-compartmental fractional model in pharmacokinetics and parameters estimation, Math. Methods Appl. Sci. 44 (2021), 11526–11536. https://doi.org/10.1002/mma.7511.

[23] I. Petráš, Fractional-order nonlinear systems: modeling, analysis and simulation, Higher Education Press Beijing and Springer-Verlag Berlin Heidelberg. (2011).

[24] K. Diethelm, A.D. Freed, On the solution of nonlinear fractional-order differential equations used in the modeling of viscoplasticity, in: F. Keil, W. Mackens, H. Voß, J. Werther (Eds.), Scientific Computing in Chemical Engineering II, Springer Berlin Heidelberg, Berlin, Heidelberg, 1999: pp. 217–224. https://doi.org/10.1007/978-3-642-60185-9_24.

[25] J.K.K. Asamoah, E. Okyere, E. Yankson, et al. Non-fractional and fractional mathematical analysis and simulations for Q fever, Chaos Solitons Fractals. 156 (2022), 111821. https://doi.org/10.1016/j.chaos.2022.111821.

[26] A. Omame, M. Abbas, C.P. Onyenegecha, A fractional-order model for COVID-19 and tuberculosis co-infection using Atangana–Baleanu derivative, Chaos Solitons Fractals. 153 (2021), 111486. https://doi.org/10.1016/j.chaos.2021.111486.

[27] A. Khan, J.F. Gómez-Aguilar, T. Saeed Khan, et al. Stability analysis and numerical solutions of fractional order HIV/AIDS model, Chaos Solitons Fractals. 122 (2019), 119–128. https://doi.org/10.1016/j.chaos.2019.03.022.

[28] M.A. Khan, A. Atangana, Modeling the dynamics of novel coronavirus (2019-nCov) with fractional derivative, Alexandria Eng. J. 59 (2020), 2379–2389. https://doi.org/10.1016/j.aej.2020.02.033.

[29] E. Bonyah, J.F. Gómez-Aguilar, A. Adu, Stability analysis and optimal control of a fractional human African trypanosomiasis model, Chaos Solitons Fractals. 117 (2018), 150–160. https://doi.org/10.1016/j.chaos.2018.10.025.

[30] A. Atangana, A. Akgül, K.M. Owolabi, Analysis of fractal fractional differential equations, Alexandria Eng. J. 59 (2020), 1117–1134. https://doi.org/10.1016/j.aej.2020.01.005.

[31] A. Atangana, S. Qureshi, Modeling attractors of chaotic dynamical systems with fractal–fractional operators, Chaos Solitons Fractals. 123 (2019), 320–337. https://doi.org/10.1016/j.chaos.2019.04.020.

[32] K.A. Abro, A. Atangana, A comparative study of convective fluid motion in rotating cavity via Atangana–Baleanu and Caputo–Fabrizio fractal–fractional differentiations, Eur. Phys. J. Plus. 135 (2020), 226. https://doi.org/10.1140/epjp/s13360-020-00136-x.

[33] S. Qureshi, A. Atangana, A.A. Shaikh, Strange chaotic attractors under fractal-fractional operators using newly proposed numerical methods, Eur. Phys. J. Plus. 134 (2019), 523. https://doi.org/10.1140/epjp/i2019-13003-7.

[34] M.H. Heydari, A. Atangana, Z. Avazzadeh, et al. Numerical treatment of the strongly coupled nonlinear fractal-fractional Schrödinger equations through the shifted Chebyshev cardinal functions, Alexandria Eng. J. 59 (2020), 2037–2052. https://doi.org/10.1016/j.aej.2019.12.039.

[35] A. Atangana, Fractal-fractional differentiation and integration: Connecting fractal calculus and fractional calculus to predict complex system, Chaos Solitons Fractals. 102 (2017), 396–406. https://doi.org/10.1016/j.chaos.2017.04.027.

[36] J.F. Zhong, N. Gul, R. Bilal, et al. A fractal-fractional order Atangana-Baleanu model for Hepatitis B virus with asymptomatic class, Phys. Scr. 96 (2021), 074001. https://doi.org/10.1088/1402-4896/abf67c.

[37] M.A. Khan, A. Atangana, E. Alzahrani, et al. The dynamics of COVID-19 with quarantined and isolation, Adv. Differ. Equ. 2020 (2020), 425. https://doi.org/10.1186/s13662-020-02882-9.

[38] M.M. El-Dessoky, M.A. Khan, Modeling and analysis of an epidemic model with fractal-fractional Atangana-Baleanu derivative, Alexandria Eng. J. 61 (2022), 729–746. https://doi.org/10.1016/j.aej.2021.04.103.

[39] B. Ghanbari, J.F. Gómez-Aguilar, Analysis of two avian influenza epidemic models involving fractal-fractional derivatives with power and Mittag-Leffler memories, Chaos. 29 (2019), 123113. https://doi.org/10.1063/1.5117285.

[40] W. Wang, M.A. Khan, Analysis and numerical simulation of fractional model of bank data with fractal–fractional Atangana–Baleanu derivative, J. Comput. Appl. Math. 369 (2020), 112646. https://doi.org/10.1016/j.cam.2019.112646.

[41] A. Atangana, M.A. Khan, Fatmawati, Modeling and analysis of competition model of bank data with fractal-fractional Caputo-Fabrizio operator, Alexandria Eng. J. 59 (2020), 1985–1998. https://doi.org/10.1016/j.aej.2019.12.032.

[42] Z. Li, Z. Liu, M.A. Khan, Fractional investigation of bank data with fractal-fractional Caputo derivative, Chaos Solitons Fractals. 131 (2020), 109528. https://doi.org/10.1016/j.chaos.2019.109528.

[43] H. Khan, R. Begum, T. Abdeljawad, M.M. Khashan, A numerical and analytical study of SE(Is)(Ih)AR epidemic fractional order COVID-19 model, Adv. Differ. Equ. 2021 (2021), 293. https://doi.org/10.1186/s13662-021-03447-0.

[44] Z. Ali, F. Rabiei, K. Shah, et al. Qualitative analysis of fractal-fractional order COVID-19 mathematical model with case study of Wuhan, Alexandria Eng. J. 60 (2021), 477–489. https://doi.org/10.1016/j.aej.2020.09.020.

[45] M.A. Abdulwasaa, M.S. Abdo, K. Shah, et al. Fractal-fractional mathematical modeling and forecasting of new cases and deaths of COVID-19 epidemic outbreaks in India, Results Phys. 20 (2021), 103702. https://doi.org/10.1016/j.rinp.2020.103702.

[46] M.B. Jeelani, A.S. Alnahdi, M.S. Abdo, et al. Mathematical modeling and forecasting of COVID-19 in Saudi Arabia under fractal-fractional derivative in Caputo sense with power-law, Axioms. 10 (2021), 228. https://doi.org/10.3390/axioms10030228.

[47] X.-P. Li, S. Ullah, H. Zahir, A. Alshehri, M.B. Riaz, B.A. Alwan, Modeling the dynamics of coronavirus with super-spreader class: A fractal-fractional approach, Results Phys. 34 (2022), 105179. https://doi.org/10.1016/j.rinp.2022.105179.

[48] Adnan, A. Ali, M. ur Rahman, et al. Investigation of time-fractional SIQR Covid-19 mathematical model with fractal-fractional Mittage-Leffler kernel, Alexandria Eng. J. 61 (2022), 7771–7779. https://doi.org/10.1016/j.aej.2022.01.030.

[49] M. Amin, M. Farman, A. Akgül, R.T. Alqahtani, Effect of vaccination to control COVID-19 with fractal fractional operator, Alexandria Eng. J. 61 (2022), 3551–3557. https://doi.org/10.1016/j.aej.2021.09.006.

[50] K. Shah, M. Arfan, I. Mahariq, et al. Fractal-fractional mathematical model addressing the situation of corona virus in Pakistan, Results Phys. 19 (2020), 103560. https://doi.org/10.1016/j.rinp.2020.103560.

[51] M.A. Almalahi, S.K. Panchal, W. Shatanawi, et al. Analytical study of transmission dynamics of 2019-nCoV pandemic via fractal fractional operator, Results Phys. 24 (2021), 104045. https://doi.org/10.1016/j.rinp.2021.104045.

[52] M. Arfan, H. Alrabaiah, M.U. Rahman, et al. Investigation of fractal-fractional order model of COVID-19 in Pakistan under Atangana-Baleanu Caputo (ABC) derivative, Results Phys. 24 (2021), 104046. https://doi.org/10.1016/j.rinp.2021.104046.

[53] Z. Ali, F. Rabiei, K. Shah, T. Khodadadi, Fractal-fractional order dynamical behavior of an HIV/AIDS epidemic mathematical model, Eur. Phys. J. Plus. 136 (2021), 36. https://doi.org/10.1140/epjp/s13360-020-00994-5.

[54] Y.-M. Li, S. Ullah, M.A. Khan, M.Y. Alshahrani, T. Muhammad, Modeling and analysis of the dynamics of HIV/AIDS with non-singular fractional and fractal-fractional operators, Phys. Scr. 96 (2021), 114008. https://doi.org/10.1088/1402-4896/ac15c3.

[55] B. Ghanbari, On the modeling of the interaction between tumor growth and the immune system using some new fractional and fractional-fractal operators, Adv. Differ. Equ. 2020 (2020), 585. https://doi.org/10.1186/s13662-020-03040-x.

[56] A. Akgül, N. Ahmed, A. Raza, et al. A fractal fractional model for cervical cancer due to human papillomavirus infection, Fractals. 29 (2021), 2140015. https://doi.org/10.1142/s0218348x21400156.

[57] J.K.K. Asamoah, Fractal–fractional model and numerical scheme based on Newton polynomial for Q fever disease under Atangana–Baleanu derivative, Results Phys. 34 (2022), 105189. https://doi.org/10.1016/j.rinp.2022.105189.

[58] H. Najafi, S. Etemad, N. Patanarapeelert, et al. A study on dynamics of CD4+ T-cells under the effect of HIV-1 infection based on a mathematical fractal-fractional model via the Adams-Bashforth scheme and Newton polynomials, Mathematics. 10 (2022), 1366. https://doi.org/10.3390/math10091366.

[59] H.W. Hethcote, Qualitative analyses of communicable disease models, Math. Biosci. 28 (1976), 335–356. https://doi.org/10.1016/0025-5564(76)90132-2.

[60] A. Atangana, S. I. Araz, New numerical scheme with newton polynomial: theory, methods, and applications, Academic Press, San Diego, 2021.

[61] A. Atangana, S.I. Araz, A novel Covid-19 model with fractional differential operators with singular and non-singular kernels: Analysis and numerical scheme based on Newton polynomial, Alexandria Eng. J. 60 (2021), 3781–3806. https://doi.org/10.1016/j.aej.2021.02.016.

[62] P. Liu, M. ur Rahman, A. Din, Fractal fractional based transmission dynamics of COVID-19 epidemic model, Computer Methods Biomech. Biomed. Eng. (2022). https://doi.org/10.1080/10255842.2022.2040489.

[63] J.-C. Zhou, S. Salahshour, A. Ahmadian, N. Senu, Modeling the dynamics of COVID-19 using fractal-fractional operator with a case study, Results Phys. 33 (2022), 105103. https://doi.org/10.1016/j.rinp.2021.105103.